Proceedings of the
Annual Stability Conference
Structural Stability Research Council
Grapevine, Texas, April 18-21, 2012

Cross-sectional stability of structural steel at elevated temperatures

M.S. Seif[1], T.P. McAllister[2]

Abstract
There is a lack of understanding of how structural systems perform under realistic, uncontrolled fires. Fire protection of steel structures is usually provided through prescriptive requirements. The development of performance-based standards and tools require explicit consideration of fire effects on structural components and systems. This paper presents a parametric study employing nonlinear material and geometric finite element analyses to model the response of wide flange steel column sections to elevated temperatures. The parametric study varied the axial load as well as the cross-sectional slenderness of three lengths of column sections exhibiting nonlinear buckling and elastic buckling, respectively. Computational results illustrate the relationship between column slenderness in the web and/or flanges, and the local and global buckling modes under varying load and temperature conditions.

1. Introduction

There is a lack of understanding of how structural systems, including connections, perform under realistic, uncontrolled fires. Fire protection of steel structures is usually provided through prescriptive requirements based on the standard fire test (ASTM, 2011) which has changed little since it was introduced in 1917. A fuller understanding of the problem will lead to the development of performance-based standards and tools that explicitly consider realistic fire loading for both the design of new buildings and assessment and retrofit of existing ones. Development of performance based standards and tools requires finite element analyses (FEA) that consider all failure modes, including buckling, at elevated temperatures. The work presented here is a first step towards achieving such a capability.

This paper presents a parametric study employing nonlinear material and geometric finite element analyses using shell elements to model the buckling response of wide flange steel column sections to elevated temperatures. The parametric study varied the axial load and temperature of three lengths of column sections that ranged from short columns with nonlinear buckling to long columns with elastic buckling Results are presented that illustrate the

[1] Structural Engineering Research Associate, ARRA Fellow, National Institute of Standards and Technology, Gaithersburg, MD 20899, mina.seif@nist.gov
[2] Research Structural Engineer, National Institute of Standards and Technology, National Institute of Standards and Technology, Gaithersburg, MD 20899, therese.mcallister@nist.gov

relationship between column slenderness in the web and/or flanges and buckling modes under varying load and temperature conditions.

2. Background

The slenderness limits of structural steel sections depend on the ratio $(E/f_y)^{0.5}$, which is used to determine which equation for critical buckling stress (inelastic or elastic buckling) applies (AISC 2010). Typically, locally slender cross-sections are avoided in the design of hot-rolled steel structural elements. Seif and Schafer (2010a) addressed the effect of increasing yield strength on local slenderness of wide flange sections. A series of simple empirical equations were developed that eliminated overly conservative slenderness criteria for high strength steels as a proposed alternative to Table B4.1 in the AISC Specification (2005).

Seif and Schafer (2009 and 2010b) investigated design criteria of three steel design specifications for wide flange sections through a FEA parametric study. The three design methods examined were the: (i) AISC (2005) method, (ii) Effective Width Method (EWM) for cold-formed steel in AISI (2007), and (iii) Direct Strength Method (DSM) in AISI (2007) Appendix 1. Results showed significant difference in the predicted capacity among the various design methods.

The performance of structural steel in fire is characterized by the thermal and mechanical properties of the steel. Thermal properties are necessary to predict effects of temperature rise in steel resulting from fire exposure and the resulting thermal expansion. Prediction of mechanical behavior requires the stress-strain relationship of steel at elevated temperatures and may be represented by such parameters as elastic modulus, yield and ultimate strengths, and creep behavior. Fig. 1 plots the temperature-dependent yield strength normalized by the room temperature yield strength, $f_y(T)/f_y$, and the normalized modulus of elasticity, $E(T)/E$, using the values presented in AISC (2010). The yield strength, f_y, sustains its value up to temperatures of about 750 ^{o}F (400 ^{o}C) before degrading, while the elastic modulus, E, starts degrading from temperatures as low as 200 ^{o}F (93 ^{o}C). When values for E and f_y at elevated temperatures were applied to the term $(E/f_y)^{0.5}$ for determining critical buckling stress in AISC (2005), unconservative predictions of critical buckling stress resulted. Takagi and Deierlein (2007) developed modified criteria for steel members at elevated temperatures that provide critical column strength for global buckling. These criteria have been incorporated into Appendix 4, Structural Design for Fire Conditions, in the AISC (2010) Specification.

Fig. 2 shows the normalized column strength $(P_{n(T)})/P_Y$ as calculated by the three steel design specifications noted above versus temperature for a W14x233 (W360x347) section with the following element thickness variations: (a) original section, (b) section with reduced flange thickness, (c) section with reduced web thickness, and (d) section with reduced flange and web thicknesses at a fixed flange-to-web thickness ratio (t_f, t_w, or both were reduced to about 20 percent of the original thickness). Differences in the column capacities among the three design methods (Fig. 2) illustrate the need to improve understanding of steel section behavior at elevated temperatures.

This paper examines the effect of elevated temperature, axial loading, and web and flange slenderness on the local and global buckling modes, including web-flange interaction, for wide-flange sections.

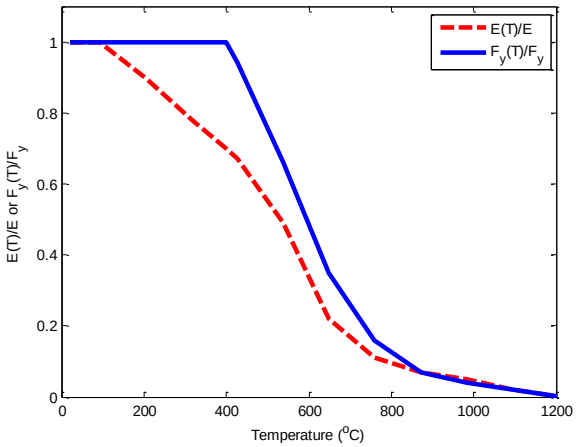

Figure 1. Material property degradation at elevated temperatures.

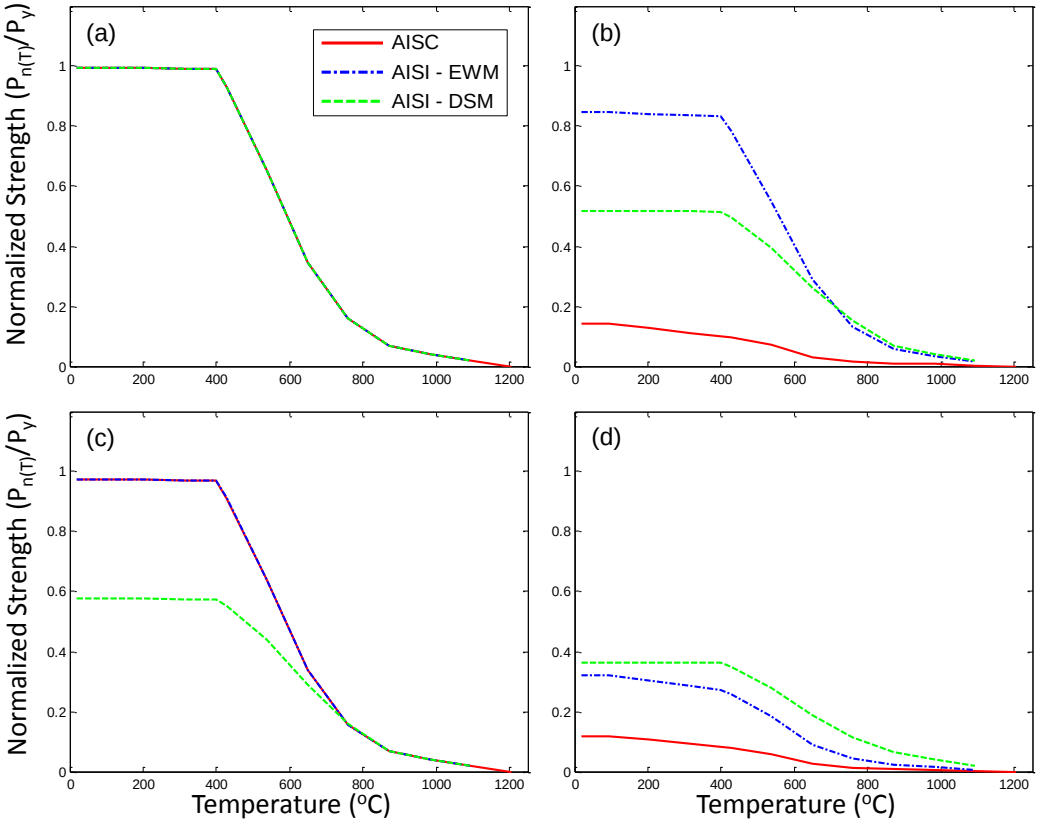

Figure 2. Normalized column strength as calculated by the three steel design methods versus temperature for a W14x233 (W360x347): (a) original section, (b) section with reduced flange thickness, (c) section with reduced web thickness, and (d) section with reduced flange and web thicknesses at a fixed flange to web thickness ratio.

3. Approach

A parametric study was conducted using nonlinear FEA to identify parameters that control the local buckling of structural steel sections under axial loads at elevated temperatures. Following the wide-flange member selection used in Seif and Schafer (2009, 2010b), W14 and W36 (W360 and W920) sections were selected for the study as representative sections for steel framed buildings. When considering flange and web thickness, the W14x233 (W360x347) and the W36x330 **(**W920x488**)** sections have approximately the average dimensions for the W14 (W360) and the W36 (W920) groups, respectively. The flange and web thicknesses were varied from the selected section geometry as part of the parametric studies. All sections were modeled with globally pinned boundary conditions. The warping degree of freedom was fixed. The axial column loads, flange and web slenderness, and column length were varied, as described in the next section.

4. Study Parameters

4.1 Section Temperature and Applied Loads

It was assumed that the elevated temperatures of the steel members were uniform throughout the cross-section and along the length. Non-uniform temperatures along the column height, with the peak temperatures near the top of the column, occur when there is a heated zone at the upper level of an enclosure from a fire located away from the column. If a fire is close to a column, the temperature will be more uniform along its height. A uniform temperature over the column length was assumed to reduce the number of parameters considered.

The buckling limit state of members under the combined effects of elevated temperature and axial loads can be evaluated either by (i) calculating the capacity of a member under a specified temperature (load approach), or (ii) calculating the critical temperature under a given axial load (temperature approach). This study used the temperature approach, which is more representative of actual fire conditions, where the temperature increases for a fixed gravity load. A gravity load was initially applied to members at room temperature (20 ºC), followed by a uniform temperature that increased until buckling failure occurred.

Column and beam members had axial loads of 0.2, 0.4, 0.6, and 0.8 of their yield capacity applied at 20 ºC. Even though beams are normally loaded normal to the longitudinal axis, for this study they were treated as axially-loaded members. The temperature was then increased at 50 ºC increments, which was linearly increased for each substep, until failure occurred. Failure is defined as a sudden increase in axial displacement, when the model typically became numerically unstable.

4.2 Web and Flange Thickness Variations

To examine the effect of web-flange interaction in wide-flange sections, four series of parametric studies were performed for varying element slenderness ratios. The flange and/or web thickness of the W14x233 **(**W360x347**)** and W36x330 **(**W920x488**)** sections were varied as indicated by the following notation:

- **FI**: only the **F**lange thickness, t_f, was varied **I**ndependently from all other dimensions
- **FR**: the **F**lange thickness, t_f, and web thickness, t_w, were varied so that the **R**atio of the flange-to-web thickness remained constant

- **WI**: only the **W**eb thickness, t_w, was varied **I**ndependently from all other dimensions

Fig. 3 shows that for the FI group, the web slenderness (h/t_w, where h is the web's clear height) is constant (compact), while the flange slenderness ($b_f/2t_f$, where b_f is the flange's width) varies from compact to non-compact. Similarly, for the WI group, the flange slenderness is constant (compact), while the web slenderness varies from compact to non-compact. The FR groups have a range of web and flange slenderness combinations. Note that λ_p and λ_r in the plot refer to the compact and non-compact slenderness limits, respectively, for web and flange elements.

Element thicknesses were varied between 0.05 in. (1.27 mm) and 3.0 in. (76.2 mm). While the range of flange and web thicknesses exceeds the range for the W14 (W360) and the W36 (W920) sections, the thickness ranges were selected to cover a range of member buckling responses.

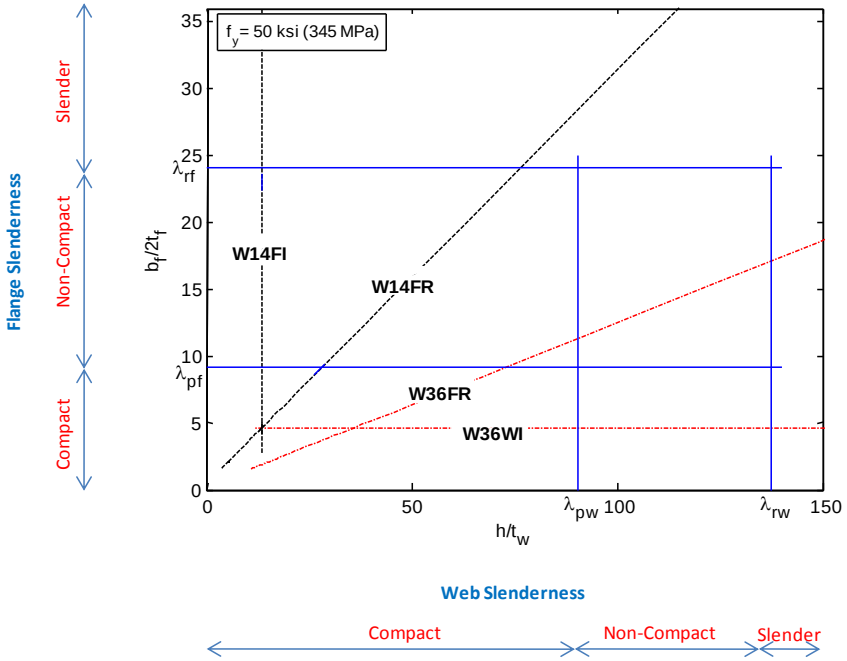

Figure 3. Variation of parameters as a function of web slenderness (h/t_w) and flange slenderness ($b_f/2t_f$). AISC compact (λ_p) and noncompact (λ_r) slenderness limits are also indicated.

4.3 Member Length Variations

Three column lengths were studied: stub (short inelastic) members, intermediate length members, and long (elastic buckling) members. The length of the stub members was determined according to the stub column definitions of the Structural Stability Research Council (Galambos 1998) to be 60 in. (1.5 m) long. To examine the effect of local-global buckling mode interaction on the strength of members, longer members were included in the FE parameter study. Two groups of analysis were chosen to be performed at lengths of 120 in. (3 m) and 240 in. (6 m) as those represent the typical heights of a single and double story column, respectively.

5. Finite Element Modeling

5.1 Mesh and Element Selection

For the structural analysis of this work, where cross-section deformation and stability are of interest, the cross-section is simplified using a two-dimensional model at the cross-section mid-

surface and employs shell finite elements to discretize the web and flanges. ANSYS shell element SHELL181 was selected for the analyses. SHELL181 is a 4-node element with six degrees of freedom at each node that is suitable for analyzing thin to moderately-thick shell structures. It is well-suited for large strain, nonlinear applications, and includes changes in shell thickness in nonlinear analyses. The mesh had one row of five shell elements across on each unstiffened element (flange) and one row of ten shell elements across each stiffened element (web).

5.2 Material Modeling

ASTM A572 Grade 50 steel was used for the study. The temperature-dependent material model is similar to that used in McAllister, et. al. (2008). The analysis used the ANSYS multi-linear isotropic hardening (MISO) model for temperature-dependent material properties, as illustrated in Fig. 4. The MISO model defines piecewise linear stress-strain curves at specified temperatures. The modulus of elasticity, E, is 29750 ksi (205119 MPa) at 20 ºC and deteriorates to about 16844 ksi (116135 MPa) at 800 ºC, and the yield stress, f_y, is 53.60 ksi (370 MPa) at 20 ºC and decreases to 5.8 ksi (40 MPa) at 800 ºC.

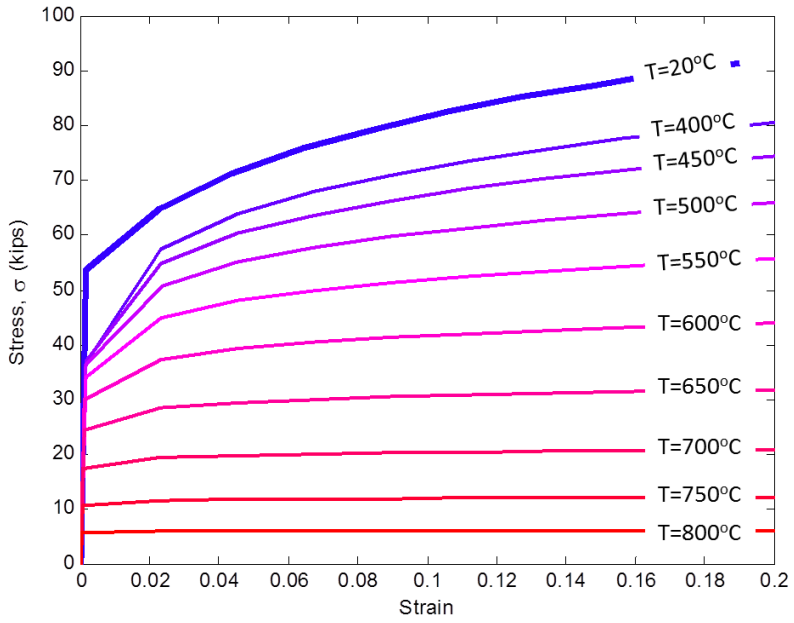

Figure 4. Temperature-dependent material model with multi-linear isotropic hardening.

5.3 Residual Stresses

Residual stresses are primarily due to differential cooling during manufacture. The classic and commonly used distribution of Galambos and Ketter (1959), as shown in Fig. 5, is employed. The compressive and tensile residual stresses are indicated by σ_c and σ_t, respectively. Similar to other researchers (e.g., Jung and White 2006), the residual stresses are defined in the finite element analysis as initial longitudinal stresses, and given as the average value across the element at its center.

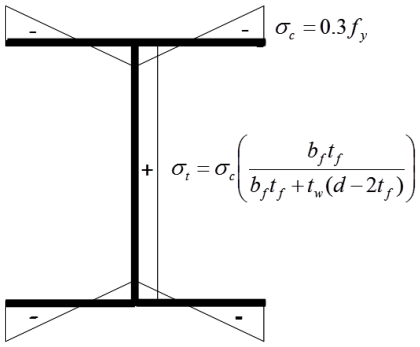

Figure 5. Residual stress distribution used for analysis as given by Galambos and Ketter (1959).

5.4 Geometric Imperfections

Geometric imperfections have an important role in any analysis involving stability as they allow FE analyses to simulate out-of-plane displacements that significantly affect member stability. Initial geometric imperfections were applied to all the members.

The stub (short) member length was selected to allow local buckling without the influence of global buckling. Therefore, global imperfections such as out-of-straightness were ignored and only local imperfections were imposed. Initial geometric imperfections were added by superposing a scaled eigenmode solution from a finite strip analysis performed on each section, using CUFSM software (Schafer and Ádány 2006). The eigenmode was scaled such that either the web out-of-flatness equals $d/150$, or the tilt in the compression flange equals b_f /150, whichever is larger (this is a commonly employed magnitude, see Kim and Lee 2002). A typical local buckling mode for a stub column and the imperfections used for its analysis are illustrated Fig. 6a, 6b, and 6c.

Longer members were selected to include global buckling modes. Initial geometric imperfections were added through linearly superposing scaled eigenmode solutions, as described. Fig. 7 shows a typical CUFSM curve, which is used to determine the half wavelengths of the local and global buckling modes. The global buckling mode is located at a half wavelength that is equal to the member unbraced length, L, while the local buckling mode is at the minima of the curve. For the purposes of this study, the local buckling half wavelength is taken as the whole number closest to the minima. The global buckling mode is scaled so that the maximum nodal displacement is equal to $L/1000$ (Kim and Lee 2002), as shown in Fig. 6d, 6e, and 6f.

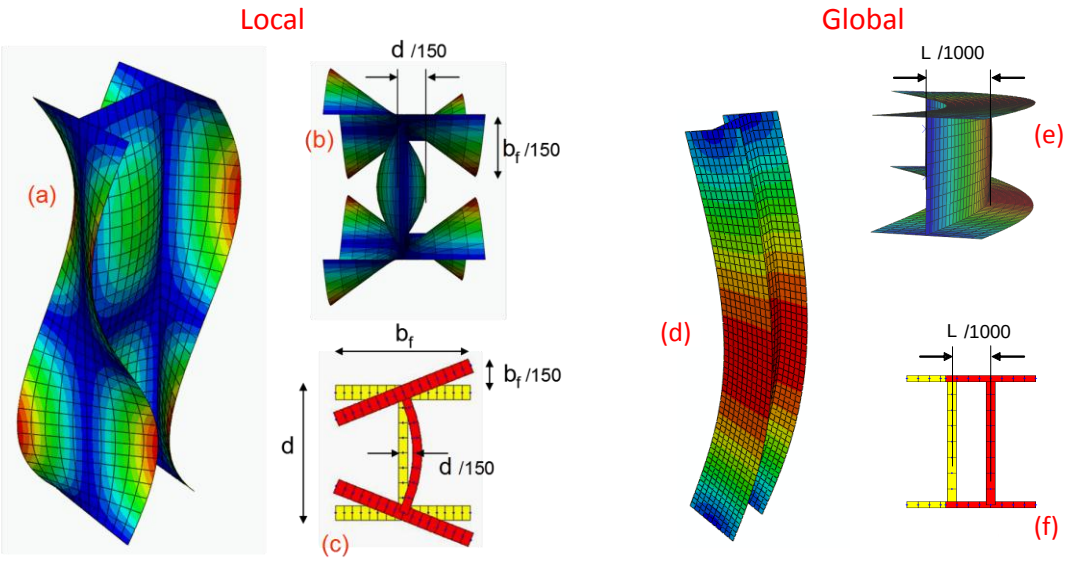

Figure 6. Typical local and global buckling modes and initial geometrical imperfections (a, d) FE 3D view, (b, e) FE axial view, and (c, f) CUFSM front view, with typical scaling factors.

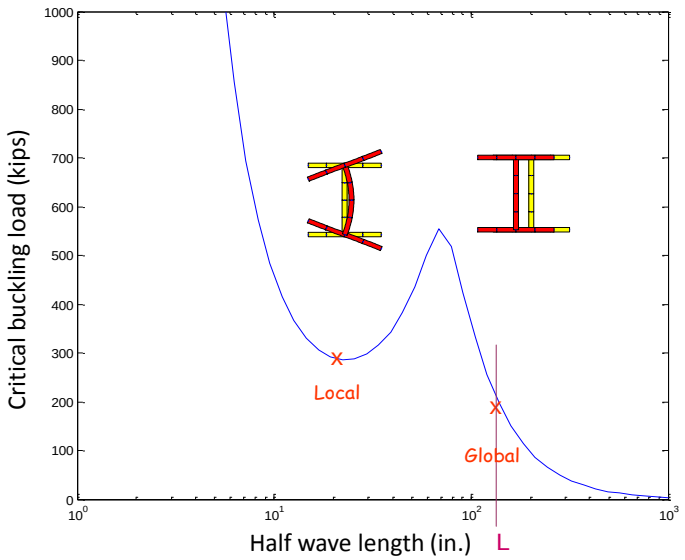

Figure 7. Typical CUFSM curve where local and global buckling modes are determined.

6. Results and Discussion

For the stub columns (length of 60 in.), Fig. 8 presents the failure temperatures versus the normalized loads for the W14 (W360) FR short length members, where the dashed line represents the original W14x233 (W360x347) member. As the web and flange slenderness increases (the elements become thinner), the curves become less linear across the normalized load range, particularly for normalized loads of 0.6 and 0.8 $P_{n(T)}/P_y$. The decreasing failure temperatures are due to the combined effects of load, web and flange slenderness, and web-flange interaction for the inelastic local buckling response.

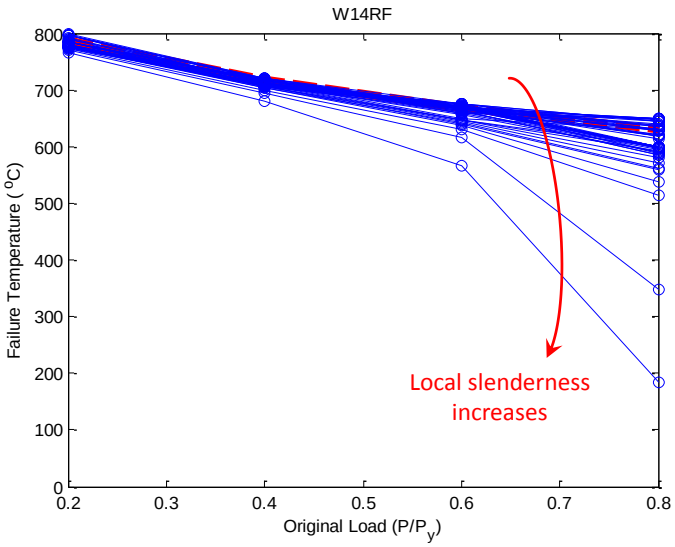

Figure 8. Failure temperatures versus the normalized loads for the W14FR short length members.

Fig. 9 presents failure temperature versus normalized load for the four groups of element thickness variation for the stub member length. For each group, results are shown for the original W14x233 (W36x330) section and for a section with the variable thickness (t_f, t_w, or both) reduced to about 20 percent of its original thickness. Similar plots are provided for the intermediate and long member lengths in Fig. 10 and Fig. 11, respectively.

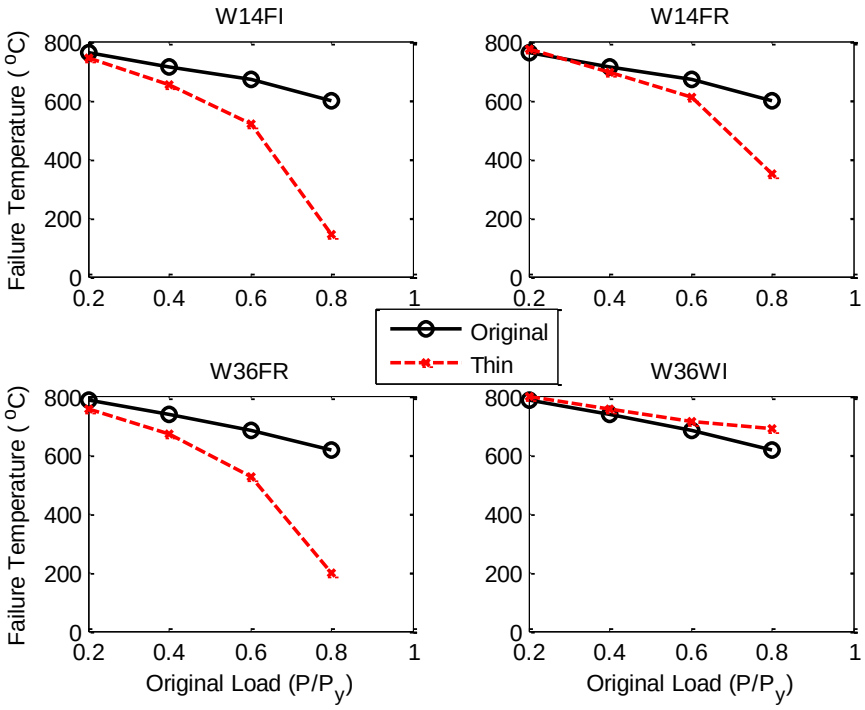

Figure 9. Failure temperatures versus the normalized loads for the short length members (60 in. (1.5 m)).

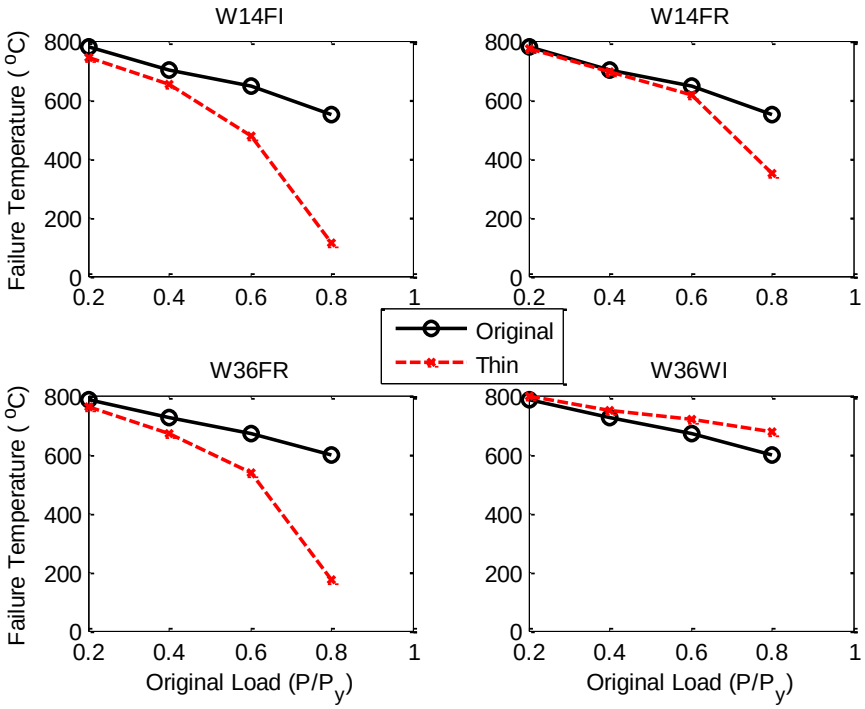

Figure 10. Failure temperatures versus the normalized loads for intermediate length members (120 in. (3 m)).

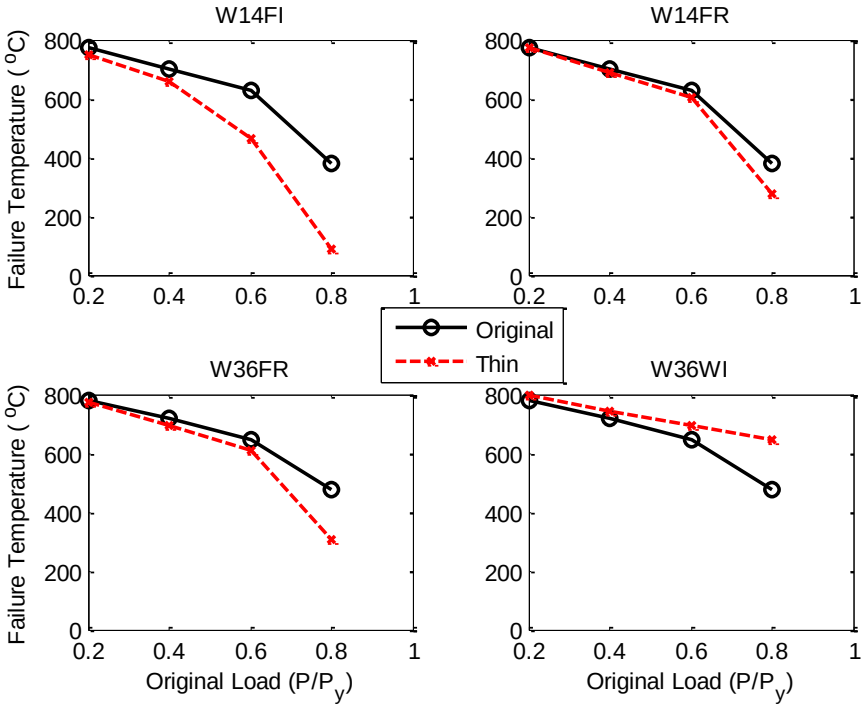

Figure 11. Failure temperatures versus the normalized loads for long length members (240 in. (6 m)).

Similar to Fig. 8, the failure temperatures for the more slender sections were reduced at higher normalized loads for the W14 (W36) FI sections, W14 (W36) FR sections, and W36 (W920) FR

sections than the original section, particularly at normalized loads of 0.6 and 0.8. However, the W36 (W920) WI sections had higher failure temperatures than the original section, particularly at normalized loads of 0.8. The thinner web element carries less of the applied section load relative to the original web element. As the web became more slender, the flanges acted as two independent columns, each buckling in a global flexure buckling mode around its own minor axis (see Fig. 13).

Fig. 12 presents the failure temperature versus the cross-sectional local slenderness (defined here as $\lambda_\ell = (f_y/f_{cr\ell})^{0.5}$, where $f_{cr\ell}$ is the member's critical buckling stress) for the W14 (W360) FR group for the four load cases and three column lengths. The column length does not play a significant role in determining the failure temperature, except for the 0.8 P_y loading case, where the long column length fails at a lower temperature.

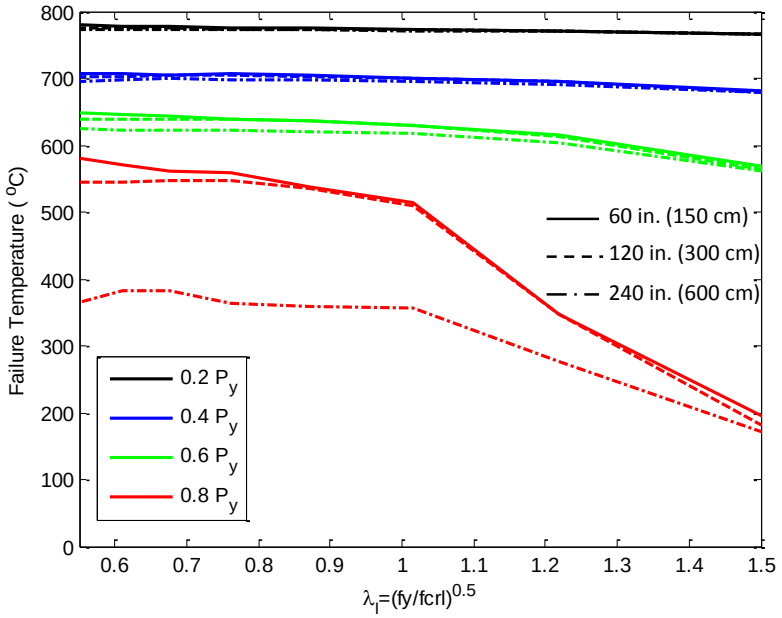

Figure 12. Failure temperatures versus the cross-sectional local slenderness for the W14FR group.

The cross-sectional local slenderness plays a key role in determining how a column fails under varying loads and temperatures. For example, for the W14(W360)FR sections, the long column with the original cross section and 0.6 P_y had nearly the same failure temperature (less than 5 percent difference) as a section with 20 percent of its original thicknesses (see Fig. 10). However, the two sections failed in completely different modes. The original column section failed in a global flexure mode, while the reduced column section failed in a local buckling mode.

Fig. 13 shows the effect of varying the flange and/or web thickness on the failure modes for the case of 120 in. (300 cm) columns under 0.4 P_y load. Failure in columns with compact flanges and webs is dominated by global flexural buckling modes (either single or double buckling waves). Failure in columns with more slender flanges and webs or with slender flanges is dominated by local buckling modes. Columns with compact flanges and slender webs have a failure mode where the flanges act as two independent columns, and each flange buckles around its own minor axis at the member end.

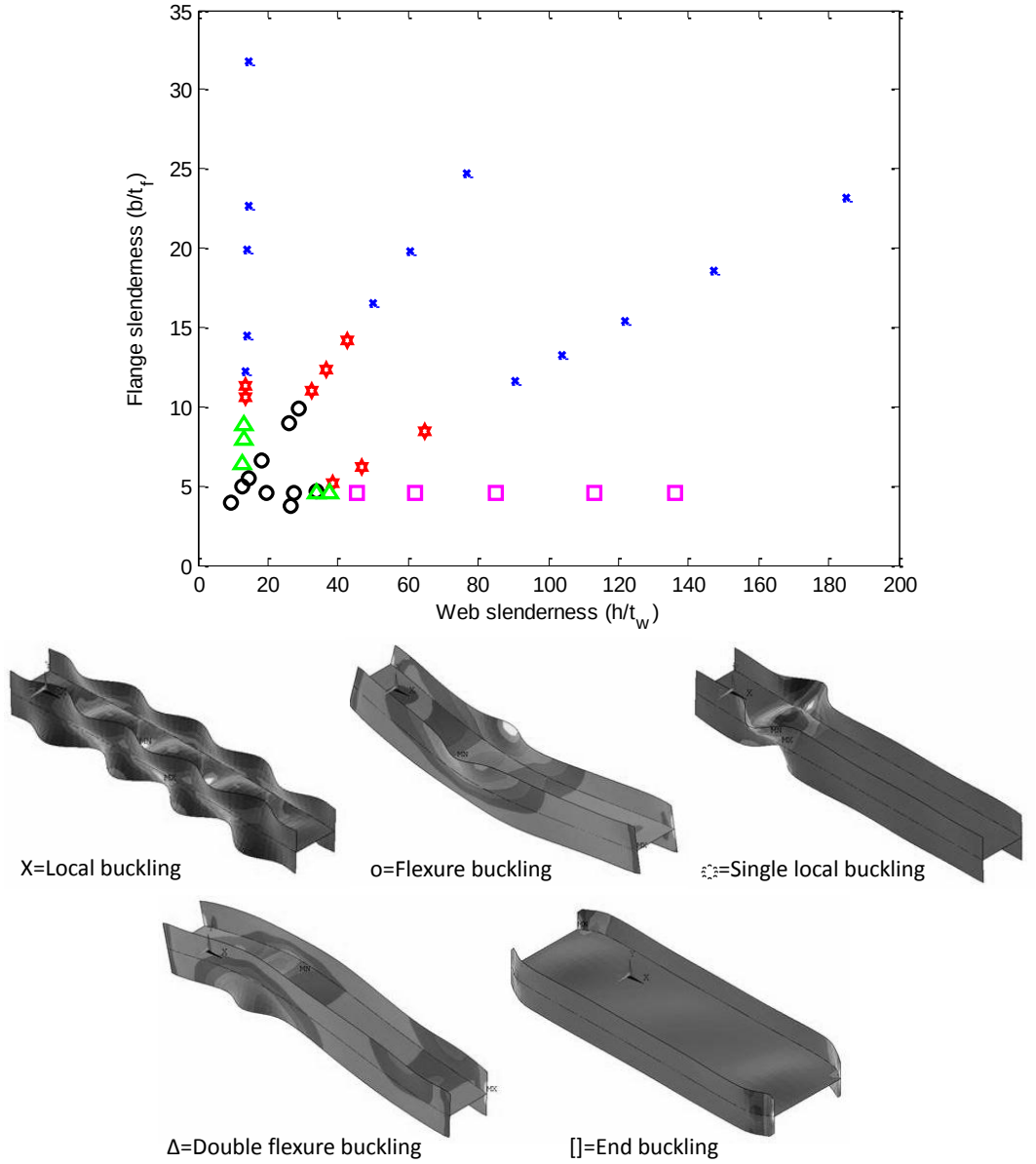

Figure 13. Effect of varying the flange and/or web slenderness on the failure modes.

The single local buckling mode was an unexpected failure mode. However, this failure mode was observed in the World Trade Center building 5 (WTC 5), which was damaged by falling debris and an uncontrolled fire on September 11, 2001. Fig. 14 shows the local buckling mode near the top of the column. Available WTC 5 structural drawings (Skilling, Helle, Chrisiansen, Robertson (1969)) indicate that the column was likely a W14x109 (W360x162) section of ASTM A36 steel with a 12 ft (3.7 m) floor to floor length.

An analysis of an A36 W14x109 (W360x162) column for uniform heating over the column length computed a single local buckling mode, similar to that shown in Fig. 13, but the failure location was not near the top of the column. A second analysis assumed that the upper portion of the column was in a hot gas layer and heated more quickly than the lower portion of the column.

To simulate such non-uniform heating conditions, the temperature was increased at four times the rate over the top quarter length of the column relative to the remainder of the column. Fig. 15 shows the failure temperatures versus the normalized loads for A36 steel and A572 steel and the associated local buckling mode near the top of the column.

Figure 14. Buckled column on the 8th floor of WTC 5 (photograph from FEMA 2002).

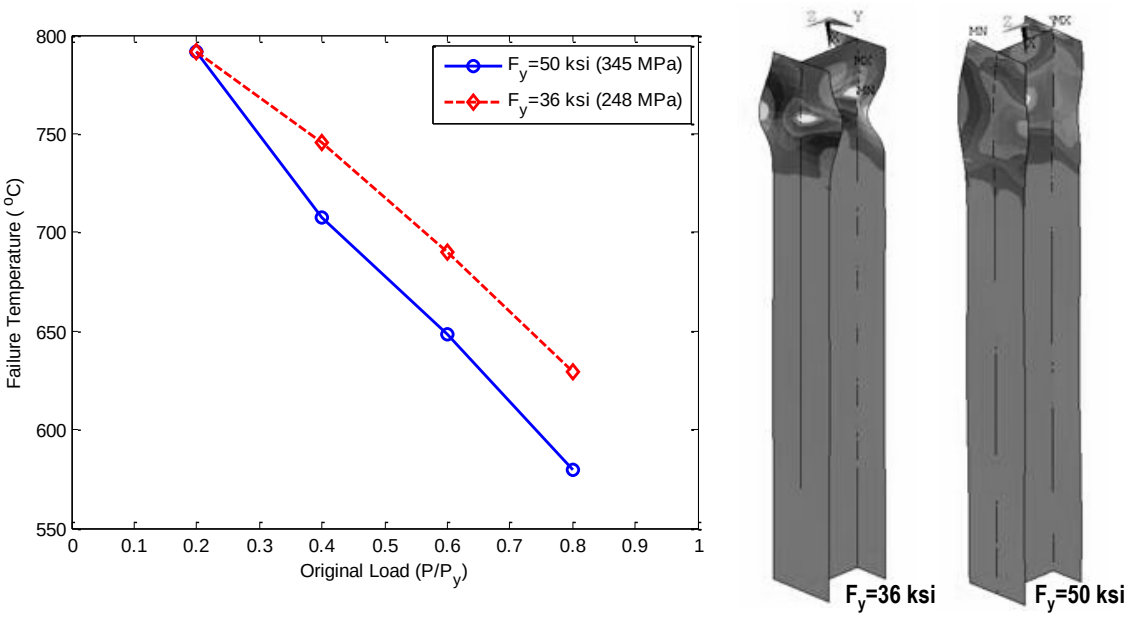

Figure 15. Failure temperatures versus the normalized loads, and failure modes for a W14 column with A36 steel and another with A572 steel.

Both columns in Fig. 15 exhibit the same local buckling failure mode but the column with 36 ksi (248 MPa) yield strength failed at higher temperatures than columns with 50 ksi (345 MPa) yield strength. This is because (i) the 50 ksi (345 MPa) columns carry larger loads as the load is normalized to P_y, and (ii) the local stability slenderness limits of structural steel sections depend on the ratio $(E/f_y)^{0.5}$. Therefore, increasing the yield strength reduces the ability of the section to remain compact.

7. Summary

This paper examines the effect of elevated temperature, axial loading, and section slenderness on the local buckling mode, including web-flange interaction, for wide-flange sections. A parametric study was conducted using nonlinear finite element analysis to identify parameters that control the local buckling of structural steel sections under axial load at elevated temperatures. The axial column loads, flange and web slenderness, and column length were varied.

The results showed the following behavior of wide-flange members at elevated temperatures:

- The cross-sectional slenderness did not have much effect on the temperature at which members buckled for loads up to 40 percent of their yield capacity.

- At loads greater than 60 percent of yield capacity, members with higher cross-sectional slenderness buckled at increasingly lower temperatures, with the exception of the W36 (W920) sections with more slender webs which buckled at higher temperatures than the original W36x330 (W920x488) section.

- Column length did not play a significant role in determining the temperature at which the sections buckled, except for the 0.8 P_y load case, where the long column length (240 in., 600 cm) failed at a much lower temperature.

- The cross-sectional local slenderness plays a key role in determining how a column buckles under varying loads and temperatures.
    - Failure in columns with compact flanges and webs is dominated by global flexural buckling modes (either single or double buckling waves).
    - Failure in columns with more slender flanges and webs or with more slender flanges is dominated by local buckling modes.
    - Columns with more slender webs have a failure mode where the flanges act as two independent columns, and each flange buckles around its own minor axis at the member end.

Based on the research conducted to date, slenderness limits appear to be a function of flange width-to-thickness ratio, web depth-to-thickness ratio, and E and f_y at elevated temperatures. Research efforts continue to use the results of this FE parameter study to define the slenderness limits of structural steel for elevated temperatures.

Disclaimer

Certain commercial software or materials are identified to describe a procedure or concept adequately; such identification is not intended to imply recommendation, endorsement, or implication by NIST that the software or materials are necessarily the best available for the purpose.

References

AISC (2005). "Specification for Structural Steel Buildings", *American Institute of Steel Construction*, One East Wacker Drive Suite 700, Chicago, IL 60601-1802, ANSI/ASIC 360-05.

AISC (2010). "Specification for Structural Steel Buildings", *American Institute of Steel Construction*, One East Wacker Drive Suite 700, Chicago, IL 60601-1802. ANSI/ASIC 360-10.

AISI (2007). "North American Specification for the Design of Cold-Formed Steel Structures", *American Iron and Steel Institute*, Washington, D.C., AISI-S100.

ASTM (2003). "Standard Specification for General Requirements for Rolled Structural Steel Bars, Plates, Shapes, and Sheet Piling", *ASTM A6/A6M-04b, American Society for Testing and Materials*, West Conshohocken, PA.

ASTM (2011), "ASTM Standard E119-11a Standard Test Methods for Fire Tests of Building Construction and Materials", *ASTM International*, West Conshohocken, PA, 2009, DOI: 10.1520/E0119-11A.

FEMA (2002). "World Trade Center building performance study: data collection, preliminary observations, and recommendations". *Federal Emergency Management Agency (FEMA) Region II*, New York, NY, 2002.

Galambos, T.V., Ketter, R.L. (1959). "Columns under combined bending and thrust", *Journal of Engineering, Mechanics Division*, ASCE 1959 85; 1–30.

Galambos, T.V. (1998). "Guide to Stability Design Criteria for Metal Structures", 5th ed., *Wiley*, New York, NY, 815-822.

Jung, S., White, D.W. (2006). "Shear strength of horizontally curved steel I-girders—finite element analysis studies", *Journal of Constructional Steel Research*, Vol 62, 2006, pp 329–342.

Kim, S., Lee, D. (2002). "Second-order distributed plasticity analysis of space steel frames", *Engineering Structures* Vol 24, 2002, 735–744.

McAllister, T., R. G. Gann, J. D. Averill, J. L. Gross, W. L. Grosshandler, J. R. Lawson, K. B. McGrattan, H. E. Nelson, W. M. Pitts, K. R. Prasad, F. H. Sadek. (2008). *Federal Building and Fire Safety Investigation of the World Trade Center Disaster: Structural Fire Response and Probable Collapse Sequence of World Trade Center Building 7*. NIST NCSTAR 1-9. National Institute of Standards and Technology. Gaithersburg, MD, October.

Schafer, B.W., Ádány, S. (2006). "Buckling analysis of cold-formed steel members using CUFSM: conventional and constrained finite strip methods", *Proceedings of the Eighteenth International Specialty Conference on Cold-Formed Steel Structures*, Orlando, FL, 39-54.

Seif, M., Schafer, B.W. (2009). "Finite element comparison of design methods for locally slender steel beams and columns", *SSRC Annual Stability Conference Proceedings*, Phoenix, AZ, April 2009, p. 69-90.

Seif, M., Schafer, B.W. (2010a). "Elastic local buckling of structural steel shapes." *Journal of Constructional Steel Research*, Vol 66, Issue 10, Oct 2010, 1232-1247.

Seif, M., Schafer, B.W. (2010b) "Design methods for local-global interaction of locally slender steel members", *SSRC Annual Stability Conference Proceedings*, May 2010, p.553-572.

Skilling, Helle, Chrisiansen, Robertson. (1969). "The World Trade Center, Drawing Book NE", Column Schedule, Skilling, Helle, Chrisiansen, Robertson Structural & Civil Engineers.

Takagi, J., Deierlein, G.G. (2007). "Strength design criteria for steel members at elevated temperatures" *Journal of Constructional Steel Research*, Vol 63, Issue 8, Aug 2007, 1036-1050.